

Alma Mater Studiorum Università di Bologna
Archivio istituzionale della ricerca

Optimization of the Zr-loading on siliceous support catalysts leads to a suitable Lewis/Bronsted acid sites ratio to produce high yields to gamma-valerolactone from furfural in one-pot

This is the final peer-reviewed author's accepted manuscript (postprint) of the following publication:

Published Version:

Garcia, A., Miguel, P.J., Ventimiglia, A., Dimitratos, N., Solsona, B. (2022). Optimization of the Zr-loading on siliceous support catalysts leads to a suitable Lewis/Bronsted acid sites ratio to produce high yields to gamma-valerolactone from furfural in one-pot. FUEL, 324, 1-10 [10.1016/j.fuel.2022.124549].

Availability:

This version is available at: <https://hdl.handle.net/11585/895431> since: 2023-05-08

Published:

DOI: <http://doi.org/10.1016/j.fuel.2022.124549>

Terms of use:

Some rights reserved. The terms and conditions for the reuse of this version of the manuscript are specified in the publishing policy. For all terms of use and more information see the publisher's website.

This item was downloaded from IRIS Università di Bologna (<https://cris.unibo.it/>).
When citing, please refer to the published version.

(Article begins on next page)

This is the final peer-reviewed accepted manuscript of:

Adrián García, Pablo J. Miguela, Alessia Ventimiglia, Nikolaos Dimitratos, Benjamín Solsona, Optimization of the Zr-loading on siliceous support catalysts leads to a suitable Lewis/Brønsted acid sites ratio to produce high yields to γ -valerolactone from furfural in one-pot, Fuel 324 (2022) 124549.

The final published version is available online at:
<https://doi.org/10.1016/j.fuel.2022.124549>

Terms of use:

Some rights reserved. The terms and conditions for the reuse of this version of the manuscript are specified in the publishing policy. For all terms of use and more information see the publisher's website.

<https://www.elsevier.com/about/policies/copyright/permissions>

This item was downloaded from IRIS Università di Bologna (<https://cris.unibo.it/>)

When citing, please refer to the published version.

Optimization of the Zr-loading on siliceous support catalysts leads to a suitable Lewis/Brønsted acid sites ratio to produce high yields to γ -valerolactone from furfural in one-pot

Adrián García^a, Pablo J. Miguel^{a,*}, Alessia Ventimiglia^{b,c}, Nikolaos Dimitratos^{b,c}, Benjamín Solsona^{a,*}

a. Departament d'Enginyeria Química, ETSE, Universitat de València, Av. Universitat, 46100, Burjassot, Valencia, Spain

b. Department of Industrial Chemistry "Toso Montanari", University of Bologna, Viale Risorgimento 4, 40136 Bologna, Italy

c. Center for Chemical Catalysis - C3, Alma Mater Studiorum Università di Bologna, Viale Risorgimento 4, 40136 Bologna, Italy

Corresponding authors: Benjamin Solsona (benjamin.solsona@uv.es)

Pablo J. Miguel (pablo.j.miguel@uv.es)

25 **Abstract:**

26 The study for the production of γ -valerolactone from furfural in one-pot has been carried out
27 using ZrO_2 supported on silica spheres. The catalysts synthesized were characterized by XRD,
28 UV-vis, HR-TEM, N_2 adsorption, IR, pyridine adsorption-IR and NH_3 -TPD in order to determine
29 their physicochemical characteristics. Both, Lewis and Brønsted acid sites are necessary to
30 produce γ -valerolactone from furfural, because they are involved in different steps of the
31 reaction. Accordingly, a reaction mechanism has been proposed. Lewis acid sites of ZrO_2
32 interacting with the $-\text{OH}$ surface groups of the siliceous spheres can generate Brønsted acid sites
33 in the supported Zr catalysts, which are absent in both pure ZrO_2 and the silica spheres. Then,
34 by controlling the amount of Zr in the supported catalysts, the relative amount of Lewis and
35 Brønsted acid sites can be optimized to obtain the highest yields to γ -valerolactone. The Zr-
36 loading of the optimal supported catalyst was ca. 7 wt.% Zr, which reached a γ -valerolactone
37 yield of 72.4 % after 8 hours at 180 °C using 2-propanol as a solvent and hydrogen donor.

38

39 **Keywords:** γ -valerolactone; furfural; Zr; silica spheres; Brønsted sites.

40

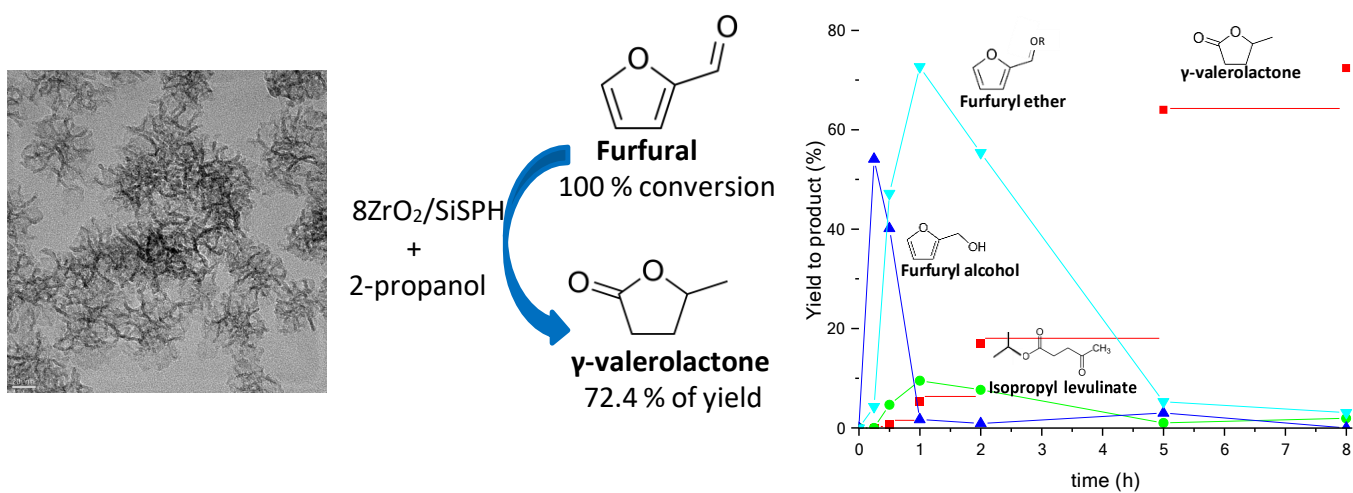
41

42

43 **Graphical abstract:**

44

45



46

47

48

49

50

51

52

53

54 **1. Introduction**

55 Research on transformation of carbon sources into valuable chemicals has increased
56 enormously in recent years due to the increasing demand for more eco-friendly transportation
57 fuels and chemical products. Moreover, this transformation of biomass has more benefits such
58 as the reduction of wastes, the lower dependency on fossil fuels and the possible mitigation of
59 the climate change [1, 2]. Furfural (FF) is one of these carbon sources, which can be transformed
60 into valuable chemicals for a sustainable production of fuels and chemicals. Thus, FF can be
61 obtained in a relatively easy way from lignocellulosic biomass, after a process of hydrolysis
62 treatment, in which mainly xylose is obtained. Then, xylose can be dehydrated using different
63 types of homogeneous or heterogeneous solid acid catalyst to finally produce FF [3, 4]. Later, FF
64 can be converted into a range of C5 and C4 molecules with high added value, such as γ -
65 valerolactone (GVL), by a multistep catalytic process. GVL is a safe, stable, renewable and
66 biodegradable chemical and it has many uses such as a solvent for biomass processing, fuel
67 additive and consumer products such as adipic acid which is a nylon precursor [5-9].

68 The most studied production process of GVL is through the hydrogenation of levulinic acid and
69 its esters using a wide variety of metallic catalysts and different types of hydrogen sources [10-
70 14]. However, the production of GVL from FF has been less studied due to its complexity,
71 because it evolves several steps in a cascade reaction process. Firstly, FF has to be transformed
72 into furfuryl alcohol (FAL) by hydrogenation and then FAL has to be transformed into alkyl
73 levulinate (AL) or levulinic acid (LA) by hydrolysis (with furfuryl ether (FE) as a reaction
74 intermediate). Once these compounds are obtained, through another hydrogenation, alkyl
75 levulinate/levulinic acid transforms into alkyl 4-hydroxy-pentanoate or 4-hydroxy-pentanoate
76 and, finally, a lactonization step produces GVL. This conversion is catalyzed by acid sites and/or
77 hydrogenating sites. Lewis acid sites (LAS) have been shown to be necessary to transform FF into
78 FAL, alkyl levulinates into alkyl 4-hydroxy-pentanoate and finally into GVL. On the other hand,

Bronsted acid sites (BAS) are necessary to transform FAL into FE and FE into alkyl levulinate and can also produce the lactonization of alkyl 4-hydroxy-pentanoate into GVL [15-18]. Unfortunately, if FF is in a high concentration (this compound but also its derivatives) can polymerize and form carbonaceous compounds, such as humins, which usually are also related with the presence of LAS. Therefore, the design of catalysts with a suitable Lewis/Brønsted ratio [19-21] has been reported to be necessary to achieve high GVL yields.

For the FF reduction to GVL a hydrogen source is required. Commonly, molecular hydrogen has been used as a H-source to transform FF into FAL [22-24]. Interestingly, transformation of FF into GVL in one pot reaction has been recently studied and developed using alcohols (such as propanol, butanol or pentanol) as both solvent and as hydrogen source to the hydrogenation reactions [25-29]. In this case, the hydrogenation process is carried out by the Meerwein-Ponndorf-Verley (MPV) reduction, where the carbonyl group on furfural is reduced to produce furfuryl alcohol and the alcohol from the MPV process is oxidized to its ketone. The same path is also followed to reduce alkyl levulinate/levulinic acid to alkyl 4-hydroxy-pentanoate [30, 31]. Finally, Lewis acid catalysts, such as metal sites, produce the etherification of alcohols and can catalyze the hydrogen transfer to produce GVL from FF using alcohols [32-34].

In order to obtain high GVL yields from FF, several heterogeneous catalysts containing both BAS and LAS have been designed. Noble and non-noble metallic based catalysts such as Ni, Au, Al, Sn, Cu or Fe and Zr, have been synthesized for the transformation of FF in order to create catalysts with acid sites [25, 35-41]. Due to its acidic properties, Zr has been the most studied non-noble metal catalyst to selectively transform FF [42-44]. The metal nanoparticles are usually supported on different materials in order to decrease the amount of added metal and to achieve a better dispersion of the metal nanoparticles in the catalysts, and eventually leading to an improvement of the catalytic activity [45]. Moreover, zeolites and acid supports are also used as acid catalysts to increase the yield to GVL [2].

For example, Winoto et al [16] synthesized a Zr-Beta catalyst after a dealumination process of the Beta zeolite and then Zr was incorporated into the beta framework. This material was finally treated with acid (heteropolytungstates of phosphotungstic acid ($\text{H}_3[\text{P}(\text{W}_3\text{O}_{10})_4]$) and silicotungstic acid ($\text{H}_4[\text{Si}(\text{W}_3\text{O}_{10})_4]$)) to introduce BAS. This way, a high GVL yield of 70 % was obtained after 24 hours at 160 °C using 2-propanol as a hydrogen donor. In another study, Zhang et al [28], designed a catalytic system to transform FF to GVL using a mixture of two different solid catalysts: i) Zr-HY, with a previous dealumination of the zeolite, and ii) Al-HY zeolites. This way, using 2-pentanol as a solvent a GVL yield of 85 % was obtained after 5 hours at 120 °C. Melero et al [19] obtained a GVL selectivity to GVL of 70 % at 170 °C after 4 hours of reaction with a bifunctional Zr–Al-beta zeolite as a catalyst.

The aim of the article is to synthesize highly active and efficient non zeolitic material. Therefore, Zr based catalysts have been developed using Al-free silica with a sphere structure as a support. Interestingly, an optimization of the Zr-loading leads to an optimal balance of both Lewis and Bronsted acid sites that not only facilitates the transformation of FF to GVL but also minimizes side reactions. Moreover, different concentrations of Zr supported on the silica support were synthesized and tested in order to improve the yield to GVL. Finally, characterization of the fresh and used catalysts has been carried out for understanding better structure-activity relationships using TPD-NH₃, FTIR spectroscopy of adsorbed pyridine, XRD, UV-vis, HR-TEM, N₂ adsorption and FTIR.

2. Experimental

2.1. Materials

Zirconium (IV) oxynitrate hydrate $\text{ZrO}(\text{NO}_3)_2 \cdot x\text{H}_2\text{O}$ (99 % purity), triethanolamine (99 % purity), hexadecyltrimethylammonium bromide (98 % purity), cyclohexane (99 % purity), tetraethyl orthosilicate (98 % purity), 2-propanol (99,5 % purity) and furfural (99 % purity) were purchased from Sigma-Aldrich.

2.2. Catalyst preparation

131 Firstly, the silica support was synthesized by the following experimental method. A solution of
132 0.36 g of triethanolamine and 10.9 g of hexadecyltrimethylammonium bromide was added and
133 mixed into 90 mL of deionized water in a beaker and the solution was under stirring at 60 °C for
134 1 hour. Another solution was prepared by mixing 32 mL of cyclohexane and 8 mL of tetraethyl
135 orthosilicate. The solution was stirred for 16 hours at 60 °C under reflux conditions. Later, the
136 mixture was heated in stirring at 90 °C for 3 hours with an aging treatment and it was cooled
137 until room temperature. The mixture was centrifuged at 8000 rpm for 15 min and washed with
138 ethanol and deionized water in order to clean the materials and remove the residual reactants.
139 The white material obtained was dried at 100 °C for 10 h and calcined for 3 h at 600 °C under
140 static air conditions. Finally, silica spheres were obtained and were labelled as SiSPH.

141 Zr was supported on silica spheres. Catalysts were synthesized by a wet impregnation method
142 using deionized water as a solvent. Different Zr concentrations were used by adding the
143 appropriate amount of zirconium nitrate ($\text{ZrO}(\text{NO}_3)_2 \cdot \text{H}_2\text{O}$). The mixture was evaporated in a hot
144 plate stirrer at 80 °C until a paste was obtained and then left in a furnace overnight at 120 °C.
145 Finally, the solid was crushed until a powder was obtained and calcined in static air at 500 °C for
146 6 h. The catalysts were labelled as $x\text{ZrO}_2/\text{SiSPH}$, being x the percentage of Zr mass of the catalyst
147 used during the synthesis, which were 4, 6, 8, 10, 12 and 20 wt.%.

148 In order to compare the catalytic performance of our Zr/spheres catalysts, a commercial silica
149 (Aerosil, Degussa, 180 m²/g) was used as a support employing the same wet impregnation
150 method. 8 wt.% was the theoretical Zr-loading selected. This catalyst was labelled as
151 $8\text{ZrO}_2/\text{Silica}$.

152 Moreover, a Zr-catalyst supported on a dealuminated zeolite Y (with a Si/Al molar ratio of 15) as
153 a support was synthesized with 8 wt.% Zr-loading (this catalyst was named as $8\text{ZrO}_2/\text{HY-15}$),
154 using the same method than in Zhang et al. [29]. In short, the support was synthesized as
155 follows. The commercial zeolite Y (from Zeolyst, Si/Al = 15 at. ratio) was treated with HNO_3 (12

M) at 80 °C for 24 hours. Later, this paste was washed with deionized water and recovered by centrifugation. The measured final Si/Al molar ratio of the dealuminated zeolite was 70. Finally, the solid was dried at 100 °C overnight.

2.3. Characterization

Catalysts were characterized by X-ray diffraction (XRD) to know the crystalline phases present in the catalysts as well as their crystallinity. The equipment used was an Enraf Nonius FR590 sealed tube diffractometer (Bruker, Delf, The Netherlands) equipped with a monochromatic Cu K α 1 source (30 mA and 40 kV).

High resolution TEM (HR-TEM) was used to analyze the catalyst structure and morphology, employing a field emission gun TECNAI G2 F20 microscope (FEI Company, Hillsboro, OR, USA) at 200 kV and a JEM 3000F microscope (JEOL, Tokyo, Japan, 300 kV). This equipment was also used for energy dispersive X-ray (EDX) and selected area electron diffraction (SAED). Firstly, a sonication treatment for 20 min was done in ethanol and deposited on a holey carbon film supported on a copper grid. TEM images were taken to observe the structure.

N₂ adsorption was undertaken at -196 °C and measured on a Micromeritics Tristar apparatus with enhanced secondary void system after outgassing at 150 °C before reaching vacuum conditions. Surface area was determined by the BET method.

Diffuse reflectance UV–Vis spectra were collected using a UV-2600 Shimadzu apparatus with a “Praying Mantis” attachment from Harrick. The sample cell was equipped with a thermocouple a heater unit and a gas flow system for “in situ” measurements.

Fourier transform infrared spectroscopy (FTIR) analysis of samples was performed using a Cary 600 spectrometer (Agilent Technologies) with a resolution of 4 cm⁻¹ and a scanning frequency of 32 min⁻¹ at room temperature. Spectra were collected in the 4000-650 cm⁻¹ region.

The Lewis and Brønsted acidity was investigated by pyridine adsorption using a Bruker Vertex 70 instrument equipped with a Pike DiffusIR cell attachment and recorded by using an MCT

182 detector after 128 scans and with a 4 cm^{-1} resolution in the region $4000\text{--}450\text{ cm}^{-1}$ to acquire in
183 situ DRIFT spectra. Samples were loaded and pre-treated in a He flow (10 mL min^{-1}) for 1 hour
184 at $300\text{ }^{\circ}\text{C}$. Spectra were acquired after the pretreatment at different temperatures ($300, 250,$
185 $200, 150, 100$ and $50\text{ }^{\circ}\text{C}$). After the pretreatment the samples were exposed to pyridine vapour
186 ($1\text{ }\mu\text{L}$) for 20 min at $50\text{ }^{\circ}\text{C}$, followed by re-evacuation at $50\text{--}300\text{ }^{\circ}\text{C}$ and IR spectra were measured
187 at the different temperatures ($50, 100, 150, 200, 250$ and $300\text{ }^{\circ}\text{C}$).

188 Ammonia thermal programmed desorption ($\text{NH}_3\text{-TPD}$) was measured with a Micromeritics
189 Autochem II 2920 analyser to investigate the strength and density of acidic sites. Samples were
190 placed in a quartz tube and pre-treated with He 20 mL min^{-1} of He at $500\text{ }^{\circ}\text{C}$ for 2 hours, then
191 reduced to $100\text{ }^{\circ}\text{C}$ and exposed to a mixture of $10\text{ }\%$ NH_3 in He (20 mL min^{-1}) for 20 min. The
192 sample was purged with He for 2 hours after flushing. The NH_3 desorption was subsequently
193 monitored using a thermal conductivity detector (TCD) at a heating rate of $10\text{ }^{\circ}\text{C min}$ up to 500
194 $^{\circ}\text{C}$ under He flow (20 mL min^{-1}).

196 2.4. Catalytic test

197 Typically, the catalytic reaction was carried out in an autoclave reactor, which was fed with 5 mL
198 of 2-propanol with a concentration of furfural of 0.05 M (0.25 mmol of FF), 0.2 g of catalyst was
199 added and the reactor was flushed three times with nitrogen for a period of 1 minute. The
200 reactor was placed on a silicon bath at $180\text{ }^{\circ}\text{C}$ under stirring for 5 hours. After reaction, the
201 reactor was cooled in an ice-bath to stop the reaction. After cooling, the mixture was filtered to
202 obtain the products in order to be analysed. ZrO_2 pure and silica spheres were tested as
203 reference catalysts to check the catalytic activity and to compare with the catalytic performance
204 of the synthesized catalysts.

205 The reaction products were analyzed by gas chromatography (GC) using a HP 5890 GC
206 instrument (Hewlett Packard, Palo Alto, CA, USA) equipped with an Agilent HP-1 column (30 m
207 $\times 0.32\text{ mm} \times 0.25\text{ }\mu\text{m}$), a FID detector working at $240\text{ }^{\circ}\text{C}$ and an injection port at $220\text{ }^{\circ}\text{C}$. The

temperature program for the chromatographic cycle was as follows: (i) 35 °C isothermal for 30 min, (ii) a heating rate of 1.5 °C min⁻¹ from 35 to 230 °C and (iii) 230 °C isothermal for 20 min. The reactions products were identified using a gas chromatography-mass spectrometry (GV-MS 5977A MSD-7890A, Agilent, Santa Clara, CA, USA).

Furfural conversion and yield to products were calculated as follows:

Conversion (%) = mols of furfural transformed/initial mols of furfural x 100

Yield (%) = mols of furfural transformed into product/initial mols of furfural x 100

3. Results

3.1. Characterization results

Table 1 presents some relevant characteristics of the catalysts synthesized. Thus, the surface area of the Zr-free silica spheres is high, exceeding 570 m²/g, which is remarkably higher than that of typical commercial silica. As expected, the addition of zirconium leads to a moderate decrease in the surface area at low Zr-loadings. Then, for Zr loadings of 12 wt.% and lower, the area decreases not more than 15%. However, in the catalyst with the highest concentration of zirconium (20ZrO₂/SiSPH) a higher decrease has been already observed compared to the pure support (33 % decrease). Finally, the sample without silica (ZrO₂) presents the lowest surface area (54.5 m² g⁻¹).

234 Table 1: Catalysts synthesized and its surface areas.

Catalyst	Support	Zr-loading (wt.%) ^a	S _{BET} (m ² /g)
SiSPH	SiSPH	0	573.9
4ZrO ₂ /SiSPH	SiSPH	4.5	533.9
6ZrO ₂ /SiSPH	SiSPH	5.6	515.0
8ZrO ₂ /SiSPH	SiSPH	6.8	484.5
10ZrO ₂ /SiSPH	SiSPH	8.9	476.4
12ZrO ₂ /SiSPH	SiSPH	12.4	484.3
20ZrO ₂ /SiSPH	SiSPH	21.3	382.8
ZrO ₂	-	n.d	54.5
Silica (commercial)	Silica (commercial)	0	180
8ZrO ₂ /Silica	Silica (commercial)	7.1	155.7

^a actual Zr-loading (wt.%) determined by chemical analysis (ICP).

236236

237 Figure 1 shows the X-ray diffraction patterns of the spheres silica support and the prepared
238 catalysts with different amounts of Zr and pure ZrO₂. For the spheres silica support, only one
239 wide diffraction peak at 2θ angle of 22 ° is detected, which proves that the support is
240 amorphous. When Zr was added, no new diffraction peaks were observed, and the intensity of
241 the peak at 2θ = 22 ° decreased. The lack of ZrO₂ diffraction peaks means either a high dispersion
242 of ZrO_x-species on the surface of the siliceous material or the presence of zirconia crystallites
243 with low crystallite size below 2 nm [46]. No diffraction peaks corresponding to ZrO₂ or a mixed
244 Zr-Si-phases were observed. In the case of pure bulk ZrO₂ catalyst good crystallinity was
245 observed, with the main diffraction peaks at 2θ = 17.5, 24.1, 28.1, 30.2, 31.6, 34.2, 34.6, 40.6,
246 50.3, 51, 60 [47], which mainly correspond to ZrO₂ in its monoclinic form (JCPDS: 37-1484) with
247 the main diffraction peaks at 2 θ = 28.1, 31.6 and 50.3. Some reflections of tetragonal ZrO₂
248248 (JCPDS 88-1007) at 2θ= 30.2, 34.5 and 51 were also observed.

249249

250250

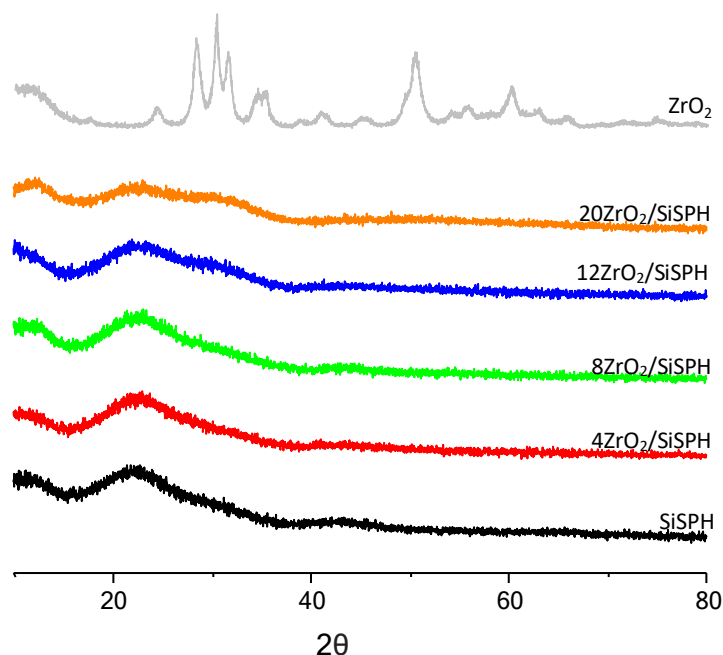


Figure 1. X-ray diffraction patterns of Zr/SiSPH catalysts, with different amounts of Zr.

In order to investigate the aggregation and coordination of the Zr-species on the support, UV-Vis analysis was carried out and the UV-vis spectra of the catalysts are shown in Figure 2. All catalysts with the presence of Zr showed a peak at 203 nm, which could be attributed to the ligand-to-metal charge transfer from O^{2-} to tetrahedral Zr^{4+} [48, 49]. This is due to the presence of highly dispersed Zr-species in the support with tetrahedral coordination. Additionally, a high intensity peak at 230 nm with a shoulder at ca. 290 nm is observed in pure ZrO_2 catalyst. These bands are due to the Zr-O-Zr charge transfer typical of bulk ZrO_2 . The peak at ca. 290 nm is also detected in the supported sample with the highest Zr-content ($20ZrO_2/SiSPH$). This suggests that in $20ZrO_2/SiSPH$ a part of Zr has been deposited on the surface of the spheres as bulk ZrO_2 , although with tiny particle size whereas, apparently, there is no bulk ZrO_2 in the remaining $ZrO_2/SiSPH$ catalysts [48, 49].

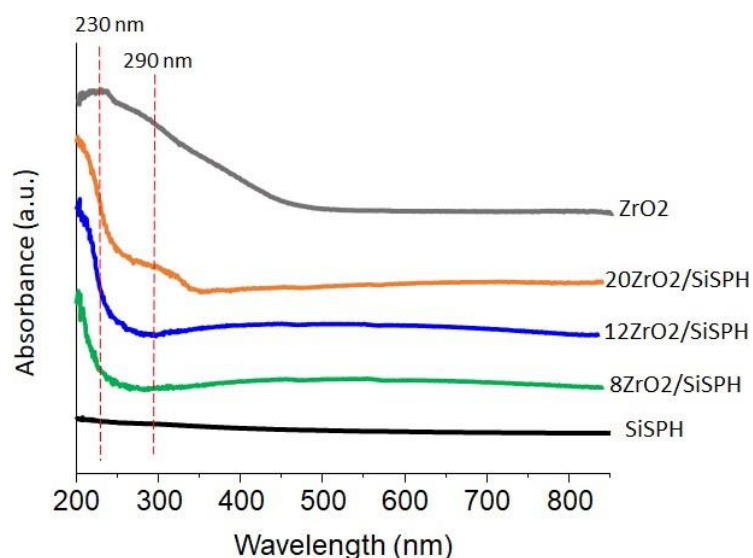


Figure 2. Absorbance UV-vis spectra of Zr/SiSPH catalysts with different amounts of Zr.

In order to study the morphology and the location of zirconium in the silica spheres, TEM analyses have been undertaken. Figure 3 shows the TEM images of the SiSPH support and the $\text{ZrO}_2/\text{SiSPH}$ catalysts with Zr-loadings of 4, 8 and 20 wt.%. It can be seen that the structure of spherical micelles of the support are highly uniform with an average diameter of 50-65 nm. Spheres with the same morphology and size are observed in the supported catalysts, confirming that the structure of the spheres remain stable after the Zr-addition. Zirconium can be observed well dispersed over the spheres surface in most of the supported catalysts. However, in the supported catalyst with the highest Zr-loading ($20\text{ZrO}_2/\text{SiSPH}$), the micelles are completely covered by zirconium oxide crystallites. Nevertheless, no isolated pure ZrO_2 agglomerations without interacting with the silica spheres have been observed.

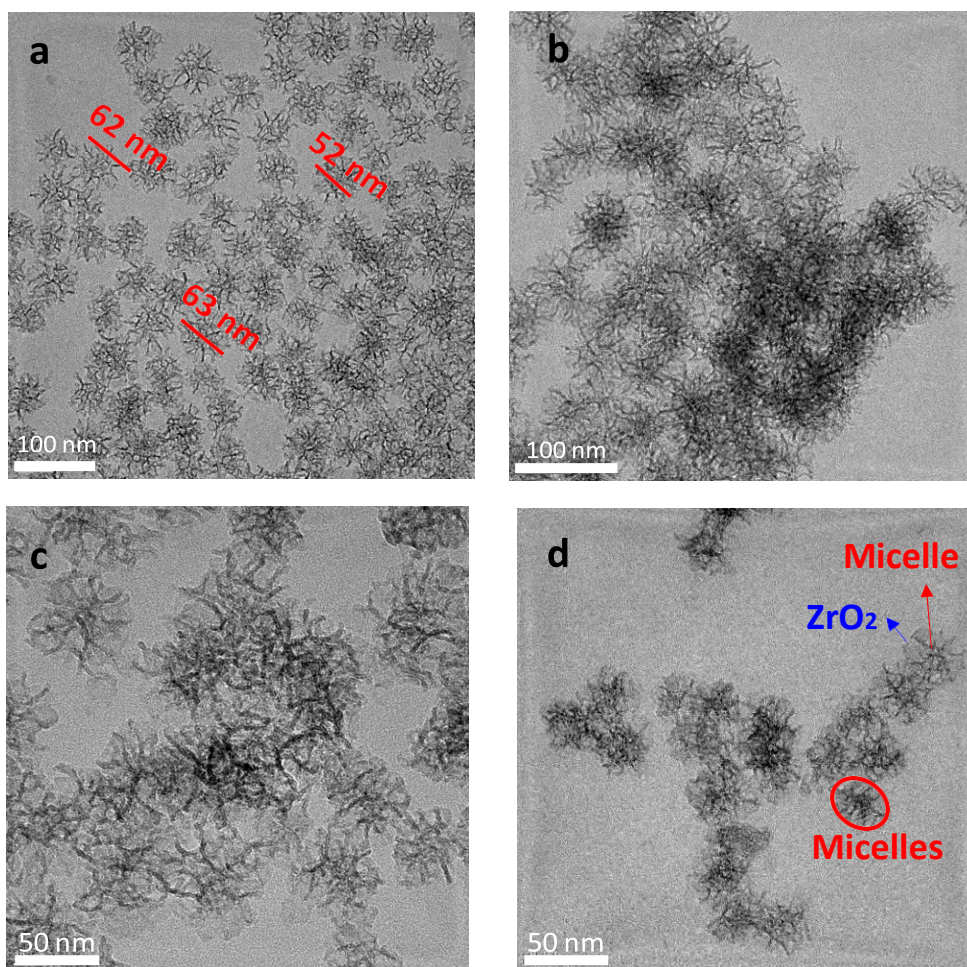


Figure 3. TEM images of SiSPH (a), 4ZrO₂/SiSPH (b), 8ZrO₂/SiSPH (c), 20ZrO₂/SiSPH (d).

FTIR analysis was carried out for all Zr/SiSPH catalysts (Figure 4). The spectra of pure ZrO₂ and the SiSPH support are also presented for comparison. The FTIR spectra of pure ZrO₂ presents a main band at 754 cm⁻¹ that is attributed to the Zr-O stretching vibrations at ZrO₂ [50]. This band is notorious in the pure ZrO₂ catalyst whereas it can be seen with very low intensity in the catalyst with the highest Zr-loading (20ZrO₂/SiSPH). In the other Zr-containing catalysts this band has not been observed, which means there is no Zr present in bulk in the catalyst and it is well dispersed on the support in agreement with the XRD data. Additionally, a peak of lower intensity at 1635 cm⁻¹ confirms the presence of adsorbed water (Zr-H₂O). This peak can be observed in pure ZrO₂ but also in the catalysts with ZrO₂. A peak at 3400 cm⁻¹ corresponding to the OH vibration [51] can be detected in all catalysts and in pure ZrO₂, but not in the Zr-free silica

spheres. These peaks in the supported $\text{ZrO}_2/\text{SiSPH}$ catalysts can be due to the presence of silanol groups (Si-O-H) or to the presence of bonded hydroxyl group on zirconium (Zr-O-H). A high intensity peak at 1100 cm^{-1} related to the vibration asymmetry of siloxane bonds (Si-O-Si) together with a peak at 800 cm^{-1} due to the vibration of symmetric Si-O-Si bonds in the framework are observed in $x\text{ZrO}_2/\text{SiSPH}$ catalysts and in the pure SiSPH support [52].

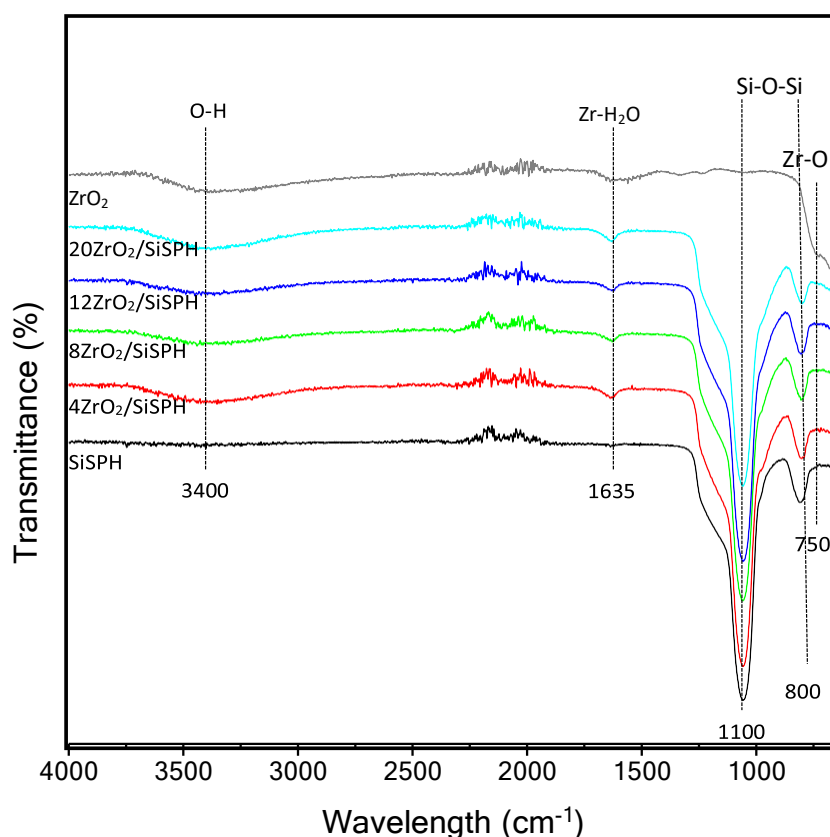
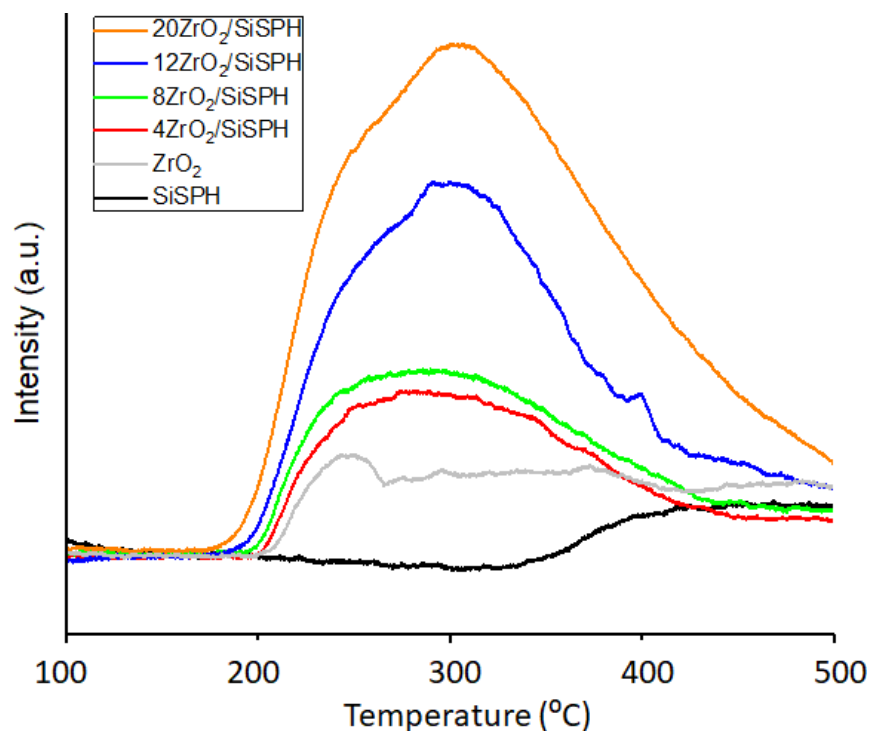


Figure 4. FTIR spectra of the support (SiSPH), the supported Zr catalysts and pure ZrO_2 .

The acid characteristics (i.e. amount of acid sites, strength and type) must be controlled in order to achieve optimal results in the catalytic reaction studied. Therefore, our catalysts have been characterized by two different techniques (NH_3 -TPD and FTIR spectroscopy of adsorbed pyridine) in order to have a detailed picture of their acidic characteristics in terms of strength of

acid sites and nature of acid sites. Figure 5 shows the NH₃-TPD profiles for all Zr/SiSPH catalysts as well as those of pure ZrO₂ and the SiSPH support.



308308

309 **Figure 5.** NH₃-TPD profiles of SiSPH support, 4ZrO₂/SiSPH, 8ZrO₂/SiSPH, 12ZrO₂/SiSPH,
310 20ZrO₂/SiSPH and pure ZrO₂.

311

312 According to this technique, the total acidity of the catalysts (Table 2) has been also determined.

313 In some occasions, three types of bands can be proposed depending of the strength of the acid

314 sites: weak, moderate and strong acidity, with bands centered at 175, 250 and 350 °C,

315 respectively [28]. However, in our TPD profiles not clear bands can be appreciated. Overall, no

316 weak acidity is observed in these catalysts as the ammonia adsorption begins in most cases at

317 ca. 200°C. In the SiSPH support, the desorption starts at 300 °C indicating that the majority of

318 the acidic sites are strong acid sites, but it has the lowest acidity per mass of catalyst (24.5 μmol

319 NH₃/g). The addition of Zr does not substantially change the proportion of different types of acid

320 sites because the NH₃-TPD profiles of the catalyst with different Zr/Si ratios are similar.

Interestingly, the total acidity increases when higher amounts of Zr is added. Then, the total acidity of 4ZrO₂/SiSPH is 87.2 $\mu\text{mol NH}_3/\text{g}$ and for 20ZrO₂/SiSPH is 155.7 $\mu\text{mol NH}_3/\text{g}$. However, a decrease of the acidity per gram of catalyst is observed for pure zirconia. This decrease in the acidity can be related to its low surface area (for pure ZrO₂ the S_{BET} is 54.5 m^2g^{-1}) if compared with the Zr/SiSPH catalysts (areas between 380 and 540 m^2g^{-1}). In fact, if determined the acidity normalized per surface area, it can be seen that the acidity increases in all cases with the Zr-loading, the pure ZrO₂ sample being the one with the highest values. The support has an acidity per area of 0.04 $\mu\text{mol NH}_3/\text{m}^2$ whereas pure ZrO₂ has a remarkably higher value of 1.43 $\mu\text{mol NH}_3/\text{m}^2$. Intermediate values are observed for the Zr/SiSPH catalysts.

Table 2. Acidity from NH₃-TPD and BAS/LAS ratio calculated with FTIR-pyr analysis.

Catalyst	Total acidity ($\mu\text{moles NH}_3/\text{g}$) ^a	Acidity per area ($\mu\text{moles NH}_3/\text{m}^2$) ^a	BAS/LAS ratio ^b
SiSPH	24.5	0.04	- ^c
4ZrO ₂ /SiSPH	87.2	0.16	n.a. ^d
8ZrO ₂ /SiSPH	99.5	0.21	0.04
12ZrO ₂ /SiSPH	117.7	0.24	0.08
20ZrO ₂ /SiSPH	155.7	0.41	0.13
ZrO ₂	78.2	1.43	0

^a determined by TPD of adsorbed ammonia; ^b determined by FTIR of adsorbed pyridine; ^c no bands corresponding to BAS or LAS have been observed; ^d n.a stands for not analysed.

FTIR spectroscopy of adsorbed pyridine (FTIR-pyr) was used to investigate the ratio of Lewis and Brønsted acid sites (LAS and BAS). Figure 6 shows the collected FTIR spectra of all catalysts, the support and pure ZrO₂. Adsorption bands at 1445, 1575 and 1600 cm^{-1} indicate the existence of coordinately bonded pyridine at LAS. The intensity of these bands decreases after increasing the evacuation temperature for mixed metal oxides, but with pure ZrO₂ this decrease is less marked,

as with other mixed metal oxides [53]. Adsorption bands at 1550 and 1640 cm^{-1} are related to the presence of coordinately bonded pyridine at BAS [17]. The SiSPH support alone was analyzed by FTIR-Py and, apparently, no peaks appeared in these frequencies related with the presence of BAS or LAS. In the remaining catalysts intensive peaks related with the presence of LAS could be clearly appreciated. These peaks became more intense with the increase in the amount of ZrO_2 added. On the other hand, a low amount of BAS was found in the Zr catalysts (low intensity of the bands at 1630 and 1540 cm^{-1}). In fact, after evacuation at 300 °C, these BAS peaks can be hardly detected. Moreover, a slight increase could be observed when the amount of ZrO_2 added was higher, which means that the amount of BAS increases when increasing the ZrO_2 loading. However, bands corresponding to BAS cannot be observed for pure ZrO_2 . This is in agreement with the absence of the Zr-OH band by FTIR (Figure 4).

Table 2 also shows the relative amount of the different acid sites (BAS/LAS ratio). This ratio has been calculated for $\text{ZrO}_2/\text{SiSPH}$ catalysts using the normalized peak areas at 1630 and 1450 cm^{-1} of the FTIR spectra after desorption at 200 °C. It can be observed that the BAS/LAS ratio increases from 0.04 for 8 $\text{ZrO}_2/\text{SiSPH}$ until 0.13 for 20 $\text{ZrO}_2/\text{SiSPH}$. Then, adding Zr to this siliceous support using this impregnation method, BAS can be generated. This is in accordance with that observed by Saito et al. [54], in which a high density of LAS and a surface with –OH groups lead to the formation of BAS on the support based on silica. Moreover, if residual surface silanol groups are present in the support (or it can be created during the synthesis method), a low concentration of BAS can be also formed as it was previously proposed in another study [34].

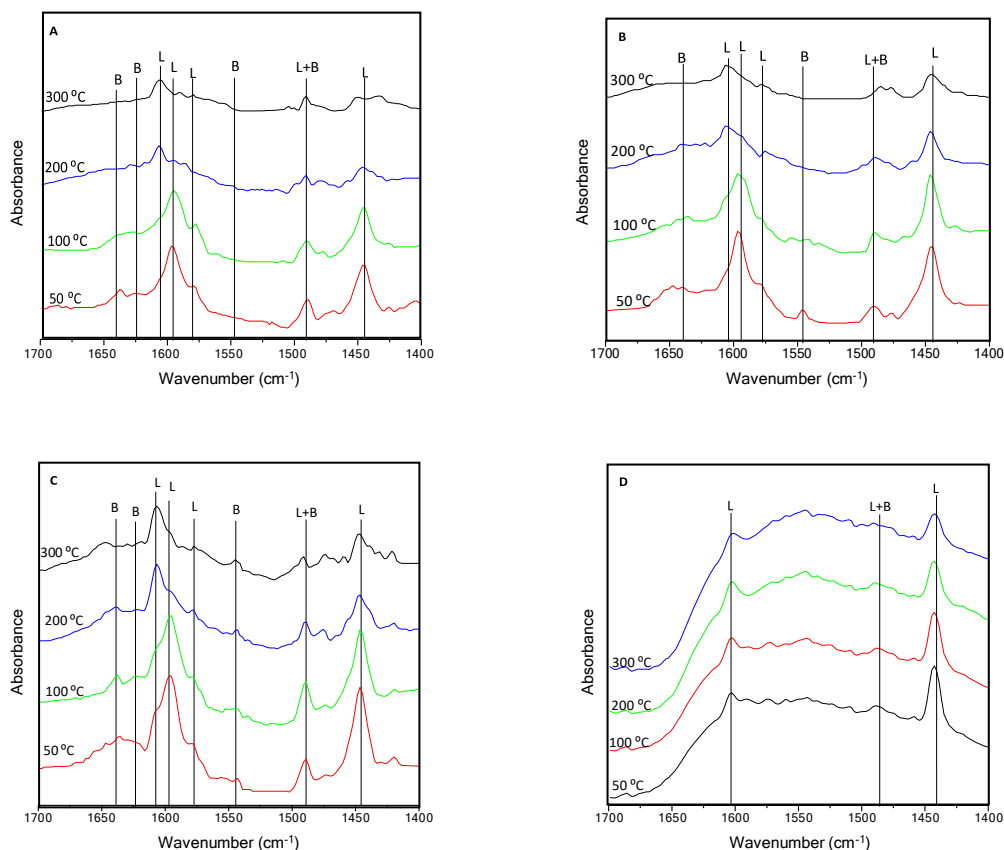


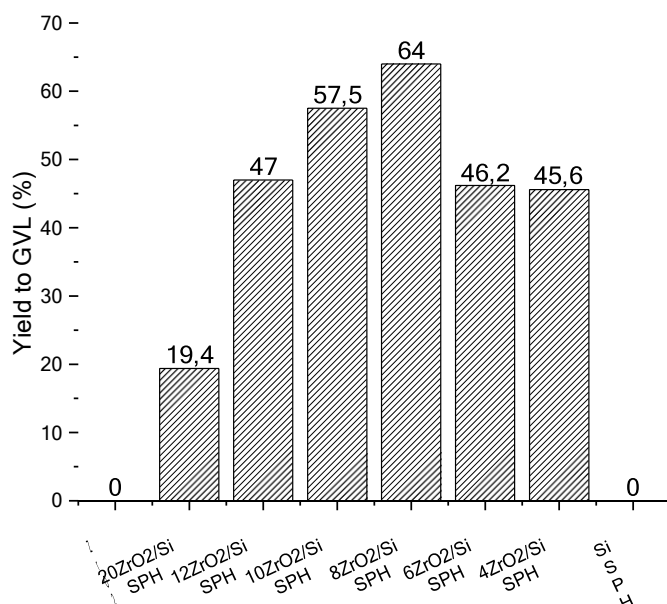
Figure 6. FTIR spectra of absorbed pyridine at different temperatures over (A) 8ZrO₂/SiSPH (B) 12ZrO₂/SiSPH (C) 20ZrO₂/SiSPH (D) ZrO₂.

Catalytic results

Catalytic experiments in the furfural transformation have been undertaken using standard reaction conditions with 2-propanol, that exerts a double role both as a solvent and as hydrogen donor. Table S1 shows the catalytic results in the furfural (FF) transformation at 180 °C and a reaction time of 5 h (remaining reaction conditions in the Experimental section) for Zr/SiSPH catalysts as well as the siliceous support and pure ZrO₂.

Interestingly, for both pure ZrO₂ and the support SiSPH not even traces of γ -valerolactone (GVL) were observed. However, all the Zr/SiSPH obtained a high yield to GVL (in all cases over 45%, except the catalyst 20ZrO₂/SiSPH), although the catalytic results vary depending on the Zr-

loading of the catalyst (Figure 7). The catalyst that had the highest yield to GVL (64 %) in these reaction conditions was that with a theoretical Zr loading of 8 wt. % (8ZrO₂/SiSPH).



376376

Figure 7. Yield to GVL from FF using xZrO₂/SiSPH catalysts, pure ZrO₂ and SiSPH support. Reactions conditions: 5 mL of 2-propanol, 0.25 mmol of FF, 0.2 g of catalyst, 180 °C, 5 h.

Therefore, based on the promising catalytic data, the 8ZrO₂/SiSPH catalyst was selected to undertake further FF transformations into GVL under the same experimental conditions, as a function of reaction time that will help to understand better the formation of primary, secondary and final products during the progress of reaction. Figure 8 shows the yield to the products with the catalyst after 15 and 30 minutes and 1, 2, 5 and additionally 8 hours of reaction at 180 °C. After 15 minutes of reaction, FF conversion was of 68.3 % (Table S2). In this case, a high yield to FAL (ca. 55%) was observed whereas low yields to FE, IPL and GVL were achieved. After 30 minutes of reaction, not only a drastic increase of the FF was observed but also a very different product distribution was found. Then, FF had been almost totally transformed (conversion > 98%). Regarding the reaction products, the yield to FAL decreased and the yield to FE increased compared to that at 15 min. Moreover, low yields to IPL and GVL were observed. The highest yield to FE was achieved after 1 hour of reaction, with a yield to FE of ca. 73% %, the yield to FAL

being only of 1.7 %. This means that FF is first transformed into FAL and later FAL reacts with 2-propanol to produce FE. After 1 hour of reaction the yield to IPL increased until ca. 10 % and the yield to GVL was still of 5 %. After 2 hours, the yield to FE decreased until 55 % whereas the yield to GVL increased until 17 %. A remarkable increase in the GVL yield was observed after 5 hours of reaction (64 %) whilst a drastic decrease of the yield to FE (ca. 5 %) took place. This suggests that FE is transformed into IPL in the hydration/ring-opening-reaction, which is the rate-determining step. The highest yield to GVL of ca. 73% was achieved after 8 hours of reaction, although the increase of the GVL yield with the time was slowed down.

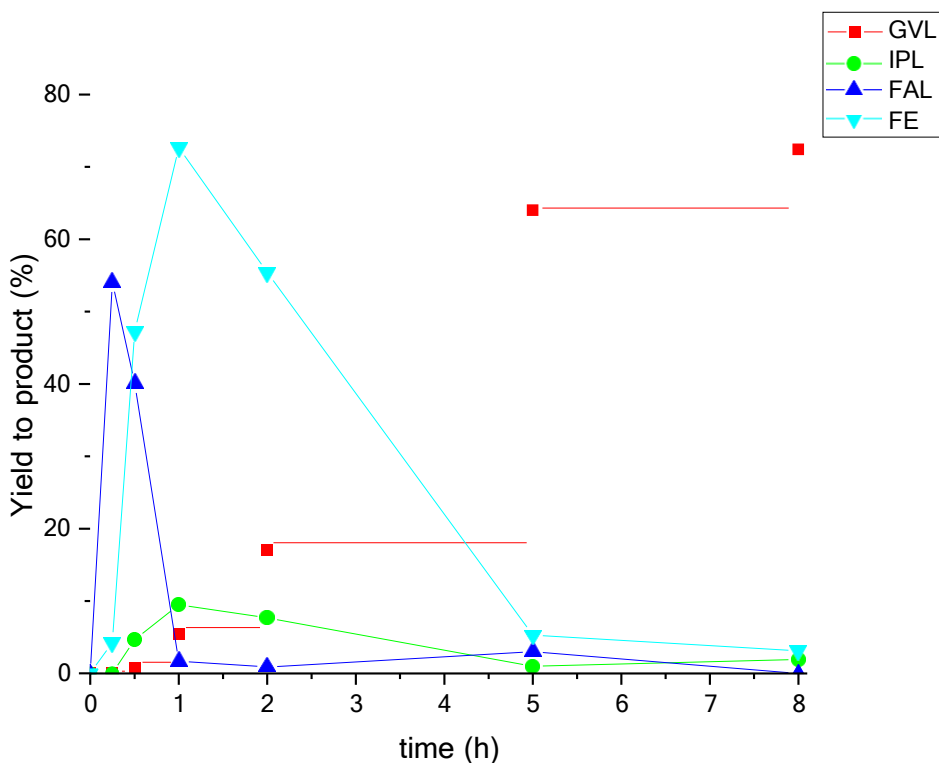


Figure 8. Yield to different products (%) at different times with catalyst 8ZrO₂/SiSPH. Reaction conditions: 5 mL of 2-propanol, 0.25 mM of FF, 0.2 g of catalyst, 180 °C.

For a proper comparison of the reactivity of the active sites of the different catalysts, new experiments using lower amounts of catalyst and lower reaction times were undertaken. Table 3 shows the values of the catalytic activity, specific activity per surface area and activity per Zr-

site. It has been observed that the support presents an extremely low reactivity that highly increases when adding zirconium. Then, the reactivity of the support is, per gram of catalyst, 50-100 times lower than those of the Zr-containing samples. Among the supported catalysts, those with intermediate Zr-loadings obtain the highest catalytic activities. If considered the actual amount of zirconium, the activity per Zr site follows a similar trend with those catalysts with low and intermediate Zr content being the most active. In this case, a drastic decrease of the activity per Zr content is observed at high Zr loadings, especially in the catalyst with the highest amount of Zr (20ZrO₂/SiSPH).

Table 3. Catalytic parameters in the furfural transformation on Zr catalysts supported on silica spheres.^a

Catalyst	Catalytic activity ^b	Specific activity ^c	Apparent TOF ^d (h ⁻¹)
SiSPH	0.3	0.06	-
4ZrO ₂ /SiSPH	15.5	3.00	32.4
6ZrO ₂ /SiSPH	26.5	5.15	43.2
8ZrO ₂ /SiSPH	34.3	7.08	46.0
10ZrO ₂ /SiSPH	38.0	7.98	38.9
12ZrO ₂ /SiSPH	28.7	5.93	21.1
20ZrO ₂ /SiSPH	20.2	5.28	8.6

^a Reaction conditions: 5 mL of 2-propanol, 0.25 mM of FF, 0.01 g of catalyst, 180 °C, reaction time = 0.25 h; ^b Catalytic activity per gram of catalyst in 10⁻³ molFF h⁻¹ g_{cat}⁻¹; ^c Specific activity is the catalytic activity normalized per surface area in 10⁻⁵ molFF h⁻¹ m⁻²; ^d Catalytic activity per mol of Zr present in the catalyst in 10⁻⁴ molFF h⁻¹ molZr⁻¹.

General remarks

Both the presence of zirconium and the silica spheres have been shown to be necessary to obtain GVL in high yield. In the case of the Zr-free SiSPH support the furfural conversion was low (below 10 %), whereas for pure ZrO₂ the conversion was very high (higher than 98 %). However, in both cases not even a small part of FF was transformed into GVL. Then, using pure ZrO₂ the main reaction products observed were furfuryl alcohol (FAL) and furfuryl ether (FE). The lack of Brønsted acid sites is very likely to be the responsible for the absence of GVL.

As it was demonstrated elsewhere [28], the presence of both Brønsted and Lewis acid sites together with relatively high reaction temperature are necessary for the cyclization of the levulinates into GVL, whereas Brønsted acid sites are required for the furan ring opening to form isopropyl levulinate (IPL). Moreover, the presence of H₂O, which is produced by etherification between furfural and 2-propanol, is necessary to transform furfuryl ether into isopropyl levulinate [17, 34, 45, 48]. This is in agreement with the absence of formation of GVL using pure ZrO₂ (only presenting LAS) although the furfural conversion was higher than 98 %.

Interestingly, using the Zr/SiSPH catalysts a notorious GVL formation was observed in all cases. The highest GVL formation was achieved employing the catalyst with an intermediate Zr-loading (8ZrO₂/SiSPH) reaching a yield to GVL of 64 %. Then, the order of GVL formation followed the sequence: 8ZrO₂/SiSPH (64%) > 10ZrO₂/SiSPH (57.5%) > 12ZrO₂/SiSPH (47%) > 6ZrO₂/SiSPH (46.2%) > 4Zr/SiSPH-30 (45.6%) > 20ZrO₂/SiSPH-5 (19.4%) > ZrO₂, SiSPH (0%). In the case of all Zr/SiSPH catalysts the main reaction product was GVL although important amounts of other compounds such as FAL, FE, IPL, levulinic acid and furfuryl acetate were also detected (Table 3).

In another study, using Zr as metal active site and a siliceous material as a support Maderuelo-Solera et al. [21] obtained the highest yield to GVL with a catalyst with a Si/Zr molar ratio of 5 and after 6 hours of reaction at 170 °C, achieving yields to GVL lower than 20 %. Interestingly, in the present work yields to GVL are remarkably higher (72.4%) than those of the previous work using similar reaction conditions. Variations in the preparation method as well as subtle changes in the reaction conditions can explain the different results.

According to our catalytic results, considering the evolution of the reaction products with the reaction time a reaction scheme has been proposed. Figure 9 represents a mechanism of reaction for the conversion of FF into GVL using our Zr/spheres catalysts. The presence of Lewis and Brønsted acid sites in these catalysts as well as the use of 2-propanol as a solvent are required for this mechanism to take place. Then, it seems to be necessary the presence of BAS apart from LAS to obtain GVL from FF, but the BAS/LAS ratio (0.04-0.08) must be controlled to

maximize the GVL formation. Therefore, an effective catalyst to transform FF into GVL must possess a high Lewis acidity and a sufficient amount of Brønsted acidity.

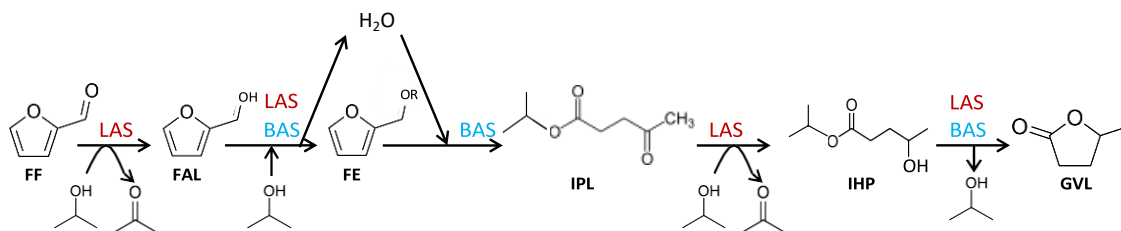


Figure 9. Proposed mechanism for one-pot conversion of FF to GVL over Zr/SiSPH catalysts. (FF: furfural, FAL: Furfuryl alcohol, IPL: isopropyl levulinate, IHP: isopropyl 4- hydroxy-pentanoate, GVL: γ-valerolactone).

As water is simultaneously produced (after the transformation of FAL into FE) and used (to transform FE into IPL, the rate-determining step) in the reaction (Figure 9), we wanted to determine the influence of its presence in the reaction media on the catalytic performance. Then, we carried out experiments with water in order to observe if it could be a limiting factor. Table 4 shows a comparison between reactions in the presence and absence of water. If water is added into the reaction, the GVL formation significantly decreased and other products were produced. This could be because water can be adsorbed into surface OH-groups at high temperatures. This adsorption into the catalyst could block the acid sites that are available to carry out the reaction to produce GVL, then decreasing its formation. As it was observed in a study of Wang et al [33], the catalyst synthesized in water was less resistant to water adsorption than other catalyst synthesized in fluoride media. This addition of water into the reaction media could result in competitive inhibition for the active sites. Moreover, in another study [25] using a Sn-Al-Beta catalysts and 2-propanol as a solvent and hydrogen donor, the yield to GVL decreased from 54.2 to 0 % when a 10 % of water was added into the reaction media.

If only water is used as a solvent, no GVL is formed and the furfural hardly can be activated (conversions of 1.3% after 5 h, see Table 4). Water is not a suitable solvent because in these conditions Zr active sites cannot take the hydrogen from the water molecule to produce the

hydrogenation of furfural. Additional experiments were undertaken with pure ethanol and conversely to water, some GVL was produced although to a lesser extent than using 2-propanol (Table S3).

Table 4. Catalytic results of the one-pot conversion of furfural using 8ZrO₂/SiSPH at different reaction times with and without addition of water.

Reaction time (h)	2-propanol: water (v:v)	FF conversion (%)	Yield to GVL (%)	Yield to IPL (%)	Yield to FAL (%)	Yield to FE (%)	Other products ^a (%)	GVL Selectivity (%)
2	10:0	≥98	46.5	10	3.4	3.5	36.7	46.5
2	9:1	84.3	1.3	10.9	7.7	0	64.4	1.5
5	10:0	≥98	64.0	0	2.9	5.3	27.8	64.0
5	9:1	≥98	7.8	35	0.9	0	55.2	7.8
5	0:10	1.3	0	0	0	0	1.3	0

^a Mols of FF transformed into other products.

It is noteworthy that in the present work high yields to GVL have been obtained without the need of a zeolitic material, just using an Al-free silica with a sphere structure as a support for Zr. The optimal Zr-loading was that with a Zr-loading of 7 wt.%. The presence of both LAS and BAS in a certain proportion has been shown to be necessary to obtain maximal GVL formation. This optimal catalyst presents both Lewis acid and Brønsted acid sites that can develop the different steps of the global FF to GVL reaction. In this case BAS/LAS ratio of 0.10 has led to the highest GVL formation. Interestingly, according to the FTIR-Py results pure silica does not present consistent Lewis sites, but when adding Zr, BAS are formed in a way that the BAS/LAS ratio increases in spite of the fact that pure ZrO₂ does not present appreciable BAS. The formation of BAS in Zr on a siliceous support as SiSPH must be caused by the presence of a high density of LAS interacting with surface –OH groups, as suggested by Saito et al. [54]. Then, conversely to what it could be expected, a higher BAS formation takes place at higher Zr-loadings in which there is a higher concentration of LAS. The decrease of GVL yields observed for high Zr-loadings, such as in the catalyst with 20 wt.% Zr, can be due to the formation of clusters of the unselective ZrO₂ particles as well as to a decrease in the surface area. Then, the optimal Zr-loading for the formation of γ-valerolactone is a trade-off between the concentration of Brønsted acid sites (low

if the Zr-loading is too low) and the presence of non-selective ZrO₂ crystallites (high if the Zr-loading is too high).

In order to compare the effectiveness of the synthesized support (SiSPH) in the FF transformation to GVL, a commercial silica and a dealuminated zeolite Y (Si/Al molar ratio of 15) (HY-15) were used as supports for Zr. For the preparation of the catalysts, the Zr loading used was that of the optimal Zr/SiSPH catalyst (8ZrO₂/SiSPH) (Table 5). By using amorphous silica as a support, 8ZrO₂/Silica, a low yield to GVL of 7.4 % was achieved. The use of a dealuminated zeolite which has been previously reported to be as one of the most efficient for this reaction [28] led to a yield to GVL of 62.7%, which is slightly lower than that obtained with 8ZrO₂/SiSPH. Interestingly, the silica spheres tested in the present article seem to be as efficient support for ZrO₂ as dealuminated Y zeolite to produce GVL from FF under these reaction conditions.

Table 5. Yield to GVL from FF using three different supports: SiSPH, commercial silica and dealuminated zeolite Y.

Catalyst	Yield (%)			
	GVL	IPL	FAL	FE
8ZrO ₂ /Silica	17.4	7.4	-	1.2
8ZrO ₂ /HY-15	62.7	-	-	3.7
8ZrO ₂ /SiSPH	64.0	1.0	2.9	5.3

Reaction conditions: 5 mL of 2-propanol, 0.25 mmol of FF, catalyst (0.2 g), 180 °C and 5 hours.

Finally, both the reproducibility of the experiments as well as the stability of the 8ZrO₂/SiSPH catalyst were studied. Then, 4 experiments were undertaken using the same reaction conditions (Table 6). The product distribution was very similar in all cases, and the yields to GVL were 64.0, 63.5, 65.9 and 62.6%, demonstrating a high reproducibility. The stability was also studied after 4 uses showing a moderate deactivation (see Figure S1).

530 Conclusions

531 γ -valerolactone can be a suitable fuel additive and a precursor of fuels and it can be produced
532 from furfural by a catalytic system developed in this work. Zr supported on silica spheres
533 catalysts have been shown to be highly efficient in the transformation of furfural into γ -
534 valerolactone, in spite of the fact that pure ZrO_2 or Zr-free silica spheres do not yield γ -
535 valerolactone in the conditions tested. The optimal catalyst presents a Zr loading of ca. 7 wt.%,
536 showing slightly higher γ -valerolactone formation than a similar catalyst using dealuminated Y
537 zeolite as a support and remarkably higher than using a conventional amorphous silica support.
538 The furfural transformation into γ -valerolactone involves reactions in cascade that require both
539 Brønsted and Lewis acid sites, being Brønsted acid sites essential to transform furfuryl alcohol
540 and furfuryl ether into isopropyl levulinate whereas Lewis acid sites are essential to obtain a
541 good hydrogenation process to γ -valerolactone. The formation of Brønsted acid sites in these
542 catalysts on pure silica has been related to the simultaneous presence of Lewis acid sites from
543 zirconia and surface $-\text{OH}$ groups of the support. Interestingly, the Zr-loading has to be controlled
544 to maximize the γ -valerolactone formation. The catalytic data showed that the amount of Zr does
545 not have to be very low, since it results in low concentrations of Brønsted acid sites, but neither
546 too high, since unselective bulk ZrO_2 is formed, therefore an optimal value of 0.04-0.08 was
547 found to be the most promising. Therefore, it is important to emphasize the elegant tuning of
548 BAS and LAS to optimize and maximize yield of GVL using Zr and Silica spheres.

549

550 Acknowledgments

551 A.G. thanks MINECO for the pre-doctoral grant (grant number PRE2018-085211). This work was
552 funded by the MAT2017-84118-C2-1-R MCIN/AEI/10.13039/501100011033/ project and FEDER
553 Una manera de hacer Europa.

554

555

557 References

- 558 [1] Zhang L, Xi G, Chen Z, Jiang D, Yu H, Wang X. Highly selective conversion of glucose into
559 furfural over modified zeolites. *Chem Eng J* 2017; 307: 868-876.
- 560 [2] Lima TM, Lima CG, Rathí AK, Gawande MB, Tucek J, Urquieta-González EA, Zbořil R, Paixão
561 MW, Varma RS. Magnetic ZSM-5 zeolite: a selective catalyst for the valorization of furfuryl
562 alcohol to γ -valerolactone, alkyl levulinates or levulinic acid. *Green Chem* 2016; 18(20): 5586-
563 5593.
- 564 [3] Guerrero-Torres A, Jiménez-Gómez CP, Cecilia JA, García-Sancho C, Franco F, Quirante-
565 Sánchez JJ, Maireles-Torres P. Ni supported on sepiolite catalysts for the hydrogenation of
566 furfural to value-added chemicals: influence of the synthesis method on the catalytic
567 performance. *Top Catal* 2019; 62(5): 535-550.
- 568 [4] Zhou N, Zhang C, Cao Y, Zhan J, Fan J, Clark JH, Zhang S. Conversion of xylose into furfural
569 over MC-SnOx and NaCl catalysts in a biphasic system. *J Clean Prod* 2021; 311: 127780.
- 570 [5] Lange JP, Vestering JZ, Haan RJ. Towards 'bio-based'Nylon: conversion of γ -valerolactone to
571 methyl pentenoate under catalytic distillation conditions. *Chem Commun* 2007; (33): 3488-
572 3490.
- 573 [6] Bond JQ, Alonso DM, Wang D, West RM, Dumesic JA. Integrated catalytic conversion of γ -
574 valerolactone to liquid alkenes for transportation fuels. *Science* 2010; 327(5969): 1110-1114.
- 575 [7] Dutta S, Iris KM, Tsang DC, Ng YH, Ok YS, Sherwood J, Clark JH. Green synthesis of gamma-
576 valerolactone (GVL) through hydrogenation of biomass-derived levulinic acid using non-noble
577 metal catalysts: A critical review. *Chem Eng J* 2019; 372: 992-1006.

578 [8] Sun Y, Wang Z, Liu Y, Meng X, Qu J, Liu C, Qu B. A review on the transformation of furfural
579 residue for value-added products. *Energies* 2020; 13(1): 21.

580 [9] García A, Sanchis R, Miguel PJ, Dejoz AM, Pico MP, López ML, Álvarez-Serrano I, García T,
581 Solsona B. Low temperature conversion of levulinic acid into γ -valerolactone using Zn to
582 generate hydrogen from water and nickel catalysts supported on sepiolite. *RSC Adv*
583 2020; 10(35): 20395-20404.

584 [10] Zhang Z. Synthesis of γ -valerolactone from carbohydrates and its
585 applications. *ChemSusChem* 2016; 9(2): 156-171.

586 [11] García A, Sanchis R, Llopis FJ, Vázquez I, Pico MP, López ML, Álvarez-Serrano I, Solsona B.
587 Ni supported on natural clays as a catalyst for the transformation of levulinic acid into γ -
588 valerolactone without the addition of molecular hydrogen. *Energies* 2020; 13(13): 3448.

589 [12] Mamun O, Walker E, Faheem M, Bond JQ, Heyden A. Theoretical investigation of the
590 hydrodeoxygenation of levulinic acid to γ -valerolactone over Ru (0001). *ACS Catal* 2017; 7(1):
591 215-228.

592 [13] Zheng J, Zhu J, Xu X, Wang W, Li J, Zhao Y, Tang K, Song Q, Qi X, Kong D, Tang Y. Continuous
593 hydrogenation of ethyl levulinate to γ -valerolactone and 2-methyl tetrahydrofuran over alumina
594 doped Cu/SiO₂ catalyst: the potential of commercialization. *Sci Rep* 2016; 6(1): 1-9.

595 [14] Nadgeri JM, Hiyoshi N, Yamaguchi A, Sato O, Shirai M. Liquid phase hydrogenation of methyl
596 levulinate over the mixture of supported ruthenium catalyst and zeolite in water. *Appl Catal A*
597 2014; 470: 215-220.

598 [15] Shao Y, Li Q, Dong X, Wang J, Sun K, Zhang L, Zhang S, Xu L, Yuan X, Hu X. Cooperation
599 between hydrogenation and acidic sites in Cu-based catalyst for selective conversion of furfural
600 to γ -valerolactone. *Fuel* 2021; 293: 120457.

601 [16] Winoto HP, Fikri ZA, Ha JM, Park YK, Lee H, Suh DJ, Jae J. Heteropolyacid supported on Zr-
602 Beta zeolite as an active catalyst for one-pot transformation of furfural to γ -valerolactone. Appl
603 Catal B 2019; 241: 588-597.

604 [17] Rao BS, Kumari PK, Koley P, Tardio J, Lingaiah N. One pot selective conversion of furfural to
605 γ -valerolactone over zirconia containing heteropoly tungstate supported on β -zeolite
606 catalyst. Mol Catal 2019; 466: 52-59.

607 [18] He J, Li H, Xu Y, Yang S. Dual acidic mesoporous KIT silicates enable one-pot production of
608 γ -valerolactone from biomass derivatives via cascade reactions. Renew Energy 2020; 146: 359-
609 370.

610 [19] Melero JA, Morales G, Iglesias J, Paniagua M, López-Aguado C. Rational optimization of
611 reaction conditions for the one-pot transformation of furfural to γ -valerolactone over Zr–Al-beta
612 zeolite: toward the efficient utilization of biomass. Ind Eng Chem Res 2018; 57(34): 11592-
613 11599.

614 [20] Sun Z, Cheng M, Li H, Shi T, Yuan M, Wang X, Jiang Z. One-pot depolymerization of cellulose
615 into glucose and levulinic acid by heteropolyacid ionic liquid catalysis. RSC Adv 2012; 2(24):
616 9058-9065.

617 [21] Maderuelo-Solera R, Richter S, Jiménez-Gómez CP, García-Sancho C, García-Mateos FJ,
618 Rosas JM, Moreno-Tost R, Cecilia JA, Maireles-Torres P. Porous SiO₂ nanospheres modified with
619 ZrO₂ and their use in one-pot catalytic processes to obtain value-added chemicals from
620 furfural. Ind Eng Chem Res 2021; 60(51): 18791-18805.

621 [22] Huang F, Li W, Lu Q, Zhu X.. Homogeneous catalytic hydrogenation of bio-oil and related
622 model aldehydes with RuCl₂ (PPh₃)₃. Chem Eng Technol 2010; 33(12): 2082-2088.

623 [23] Gowda AS, Parkin S, Ladipo FT. Hydrogenation and hydrogenolysis of furfural and furfuryl
624 alcohol catalyzed by ruthenium (II) bis (diimine) complexes. *Appl Organomet Chem* 2012; 26(2):
625 86-93.

626 [24] Yan X, Zhang G, Zhu Q, Kong X. CuZn@ N-doped graphene layer for upgrading of furfural to
627 furfuryl alcohol. *Mol Catal* 2022; 517: 112066.

628 [25] Winoto HP, Ahn BS, Jae J. Production of γ -valerolactone from furfural by a single-step
629 process using Sn-Al-Beta zeolites: Optimizing the catalyst acid properties and process
630 conditions. *J Ind Eng Chem* 2016; 40: 62-71.

631 [26] Bui L, Luo H, Gunther WR, Román-Leshkov Y. Domino reaction catalyzed by zeolites with
632 Brønsted and Lewis acid sites for the production of γ -valerolactone from furfural. *Angewandte*
633 *Chemie* 2013; 125(31): 8180-8183.

634 [27] Yu Z, Lu X, Liu C, Han Y, Ji N. Synthesis of γ -valerolactone from different biomass-derived
635 feedstocks: Recent advances on reaction mechanisms and catalytic systems. *Renew Sustain*
636 *Energy Rev* 2019; 112: 140-157.

637 [28] Zhang H, Yang W, Roslan II, Jaenicke S, Chuah GK. A combo Zr-HY and Al-HY zeolite catalysts
638 for the one-pot cascade transformation of biomass-derived furfural to γ -valerolactone. *J Catal*
639 2019; 375: 56-67.

640 [29] Zhu S, Xue Y, Guo J, Cen Y, Wang J, Fan W. Integrated conversion of hemicellulose and
641 furfural into γ -valerolactone over Au/ZrO₂ catalyst combined with ZSM-5. *ACS Catal* 2016; 6(3):
642 2035-2042.

643 [30] Koehle M, Lobo RF. Lewis acidic zeolite Beta catalyst for the Meerwein–Ponndorf–Verley
644 reduction of furfural. *Catal Sci Technol* 2016; 6(9): 3018-3026.

645 [31] Assary, R. S., Curtiss, L. A., & Dumesic, J. A. (2013). Exploring Meerwein–Ponndorf–Verley
646 reduction chemistry for biomass catalysis using a first-principles approach. *ACS Catalysis*, 3(12),
647 2694-2704.

648 [32] Li W, Li M, Liu H, Jia W, Yu X, Wang S, Zeng X, Sun Y, Wei J, Tang X, Lin L. Domino
649 transformation of furfural to γ -valerolactone over SAPO-34 zeolite supported zirconium
650 phosphate catalysts with tunable Lewis and Brønsted acid sites. *Mol Catal* 2021; 506: 111538.

651 [33] Wang J, Okumura K, Jaenicke S, Chuah GK. Post-synthesized zirconium-containing beta
652 zeolite in Meerwein–Ponndorf–Verley reduction: Pros and cons. *Appl Catal A* 2015; 493: 112-
653 120.

654 [34] Iglesias J, Melero JA, Morales G, Paniagua M, Hernández B, Osatiashtiani A, Lee AF, Wilson
655 K. ZrO₂-SBA-15 catalysts for the one-pot cascade synthesis of GVL from furfural. *Catal Sci Technol*
656 2018; 8(17): 4485-4493.

657 [35] Nandi S, Saha A, Patel P, Khan NUH, Kureshy RI, Panda AB. Hydrogenation of furfural with
658 nickel nanoparticles stabilized on nitrogen-rich carbon core–shell and its transformations for the
659 synthesis of γ -valerolactone in aqueous conditions. *ACS Appl Mater interfaces* 2018; 10(29):
660 24480-24490.

661 [36] Yan K, Chen A. Selective hydrogenation of furfural and levulinic acid to biofuels on the
662 ecofriendly Cu–Fe catalyst. *Fuel* 2014; 115: 101-108.

663 [37] Song S, Di L, Wu G, Dai W, Guan N, Li L. Meso-Zr-Al-beta zeolite as a robust catalyst for
664 cascade reactions in biomass valorization. *Appl Catal B* 2017; 205: 393-403.

665 [38] Antunes MM, Lima S, Neves P, Magalhães AL, Fazio E, Fernandes A, Neri F, Silva CM, Rocha
666 SM, Ribeiro MF, Pillinger M, Urakawa A, Valente AA. One-pot conversion of furfural to useful

667 bio-products in the presence of a Sn, Al-containing zeolite beta catalyst prepared via post-
668 synthesis routes. J Catal 2015; 329: 522-537.

669 [39] Zhou C, Xiao Y, Xu S, Li J, Hu C. γ -Valerolactone production from furfural residue with formic
670 acid as the sole hydrogen resource via an integrated strategy on Au-Ni/ZrO₂. Ind Eng Chem Res
671 2020; 59(39): 17228-17238.

672 [40] Peng Q, Wang H, Xia Y, Liu X. One-pot conversion of furfural to gamma-valerolactone in the
673 presence of multifunctional zirconium alizarin red S hybrid. Appl Catal A 2021; 621: 118203.

674 [41] Kim KD, Kim J, Teoh WY, Kim JC, Huang J, Ryoo R. Cascade reaction engineering on zirconia-
675 supported mesoporous MFI zeolites with tunable Lewis–Brønsted acid sites: A case of the one-
676 pot conversion of furfural to γ -valerolactone. RSC Adv 2020; 10(58): 35318-35328.

677 [42] Gao L, Li G, Sheng Z, Tang Y, Zhang Y. Alkali-metal-ions promoted Zr-Al-Beta zeolite with
678 high selectivity and resistance to coking in the conversion of furfural toward furfural alcohol. J
679 Catal 2020; 389: 623-630.

680 [43] Ye, L., Han, Y., Bai, H., & Lu, X. HZ-ZrP catalysts with adjustable ratio of Brønsted and Lewis
681 acids for the one-pot value-added conversion of biomass-derived furfural. ACS Sustain Chem
682 Eng 2020; 8(19): 7403-7413.

683 [44] Morandi S, Manzoli M, Chan-Thaw CE, Bonelli B, Stucchi M, Prati L, Stormer H, Wang W,
684 Wang D, Pabel M, Villa, A. Unraveling the effect of ZrO₂ modifiers on the nature of active sites
685 on AuRu/ZrO₂ catalysts for furfural hydrogenation. Sustain Energy Fuels 2020; 4(3): 1469-1480.

686 [45] García-Sancho C, Jiménez-Gómez CP, Viar-Antuñano N, Cecilia JA, Moreno-Tost R, Mérida-
687 Robles JM, Requies J, Maireles-Torres P. Evaluation of the ZrO₂/Al₂O₃ system as catalysts in the
688 catalytic transfer hydrogenation of furfural to obtain furfuryl alcohol. Appl Catal A 2021; 609:
689 117905.

690 [46] Musyarofah, Soontaranon S, Limphirat W, Pratapa S. XRD, WAXS, FTIR, and XANES studies
691 of silica-zirconia systems. *Ceram Int* 2019; 45(12): 15660-15670.

692 [47] Rauta PR, Manivasakan P, Rajendran V, Sahu BB, Panda BK, Mohapatra P. Phase
693 transformation of ZrO₂ nanoparticles produced from zircon. *Phase Transit* 2012; 85(1-2): 13-26.

694 [48] Li X, Yuan X, Xia G, Liang J, Liu C, Wang Z, Yang W. Catalytic production of γ -valerolactone
695 from xylose over delaminated Zr-Al-SCM-1 zeolite via a cascade process. *J Catal* 2020; 392: 175-
696 185.

697 [49] Ramanathan A, Castro Villalobos MC, Kwakernaak C, Telalovic S, Hanefeld U. Zr-TUD-1: A
698 lewis acidic, three-dimensional, mesoporous, zirconium-containing catalyst. *Chem Eur J*
699 2008; 14(3): 961-972.

700 [50] Elmadani AA, Radović I, Tomić NZ, Petrović M, Stojanović DB, Heinemann RJ, Radojević V.
701 Hybrid denture acrylic composites with nanozirconia and electrospun polystyrene fibers. *PloS*
702 *one* 2019; 14(12): e0226528.

703 [51] Li KM, Jiang JG, Tian SC, Chen XJ, Yan F. Influence of silica types on synthesis and
704 performance of amine–silica hybrid materials used for CO₂ capture. *J Phys Chem C* 2014; 118(5):
705 2454-2462.

706 [52] Wardhani GAPK, Nurlela N, Azizah M. Silica content and structure from corncob ash with
707 various acid treatment (HCl, HBr, and Citric Acid). *Molekul* 2017; 12(2): 174-181.

708 [53] Carniti P, Gervasini A, Bossola F, Dal Santo V. Cooperative action of Brønsted and Lewis acid
709 sites of niobium phosphate catalysts for cellobiose conversion in water. *Appl Catal B* 2016; 193:
710 93-102.

711 [54] Saito M, Aihara T, Miura H, Shishido T. Brønsted acid property of alumina-based mixed-
712 oxides-supported tungsten oxide. *Catal Today* 2021; 375: 64-69.